Title
Glioma cells display complex cell surface topographies that resist the actions of cytolytic effector lymphocytes.

Journal
Journal of immunology (Baltimore, Md. : 1950), 185(8)

ISSN
0022-1767

Authors
Hoa, Neil
Ge, Lisheng
Kuznetsov, Yurii
et al.

Publication Date
2010-10-01

DOI
10.4049/jimmunol.1001526

Glioma Cells Display Complex Cell Surface Topographies That Resist the Actions of Cytolytic Effector Lymphocytes

Neil Hoa,* Lisheng Ge,* Yurii Kuznetsov,† Alex McPherson,† Andrew N. Cornforth,‡ Jimmy T. H. Pham,§ Michael P. Myers,§ Nabil Ahmed,¶ Vita S. Salsman,¶ Lawrence S. Lamb, Jr.,‖ Joscelyn E. Bowersock,‖ Yuanjie Hu,# Yi-Hong Zhou,#, and Martin R. Jadus*,†††,‡‡**

Gliomas are invasive cancers that resist all forms of attempted therapy. Immunotherapy using Ag-pulsed dendritic cells has improved survival in some patients. We present evidence that another level of complexity may also contribute to lack of responses by the lymphocytes toward gliomas. Atomic force microscopy of four different glioma types—human U251 and rat T9 and F98 glioma cells, including freshly isolated human glioblastoma multiforme neurosphere cultures (containing "stem cell-like cells")—revealed a complex surface topography with numerous microvilli and filopodia. These structures were not found on other cell types. Electron microscopy and immunofluorescence microscopy of glioma cells confirmed that microvilli are present. U251 cells with microvilli resisted the cytolytic actions of different human effector cells, (lymphokine-activated killer cells, γδ T cells, conventional CTLs, and chimeric Ag-receptor–redirected T cells) better than their nonmicrovilli-expressing counterparts. Killer lymphocytes released perforin, which was detected within the glioma's microvilli/filopodia, indicating these structures can receive the cytolytic effector molecules, but cytotoxicity is suboptimal. Air-dried gliomas revealed nodes within the microvilli/filopodia. The microvilli that penetrated 0.4-μm transwell chamber's pores resisted the actions of CTLs and physical damage. Those nodelike structures may represent a compartmentalization that resists physical damage. These microvilli may play multiple roles in glioma biology, such as invasion and resistance to lymphocyte-mediated killing. ***The Journal of Immunology*****, 2010, 185: 4793–4803.**

Glioblastoma multiforme (GBM) are aggressive and lethal cancers. About 20,000 Americans each year are diagnosed with GBM. This cancer is almost always fatal within 5 y (2010 Central Brain Tumor Registry; http://www.braintumor.org). These cancers are very invasive, which contributes to their resistance to be cured by surgical resection and directed radiation therapy. Immunotherapy is an attractive approach for the treatment of GBM, because it allows the massive infusion or intracranial placement of ex vivo activated lymphocytes. A variety of cell types (i.e., CTLs, chimeric Ag-receptor–redirected T cells [CAR-T cells], lymphokine reactive killer cells, allogeneic mixed lymphocyte reactive T cells, and γδ T cells) show very good cytotoxic effector function against glioma cells in vitro (1–8). The clinical application of these cells has not improved survival for most patients with GBM, as would be predicted from their respective in vitro cytolytic assays.

The known requirements for initiation of immune responses in the brain are more stringent than those cancers found elsewhere in the body because of the relative isolation from the systemic circulation via the blood–brain barrier (9), poor expression of HLA Ags on brain cells (10), and unconventional lymphatic drainage (11). Local microglial cells can process and present tumor-associated Ags to CTL (12–14). These effector lymphocytes then infiltrate the tumor (3). CTLs fail to generate an effective immune response to the GBM, as evidenced by improved survival. Immunosuppressive cytokines, inhibitory factors, monocyte-derived suppressor cells, T regulatory cells, and other factors limit the immune response via multiple mechanisms that inhibit dendritic cell (DC) maturation, Ag presentation, and T cell activation (15–31). Therefore, any successful immunotherapeutic approach to GBM must overcome the challenges of access to the tumor, poor immunogenicity of the tumor, and the immunosuppressive effect of GBM-derived cytokines.

The physical interaction between cytolytic lymphocytes and glioma-associated ligands was described within one study (32). We now present evidence that another level of complexity may also contribute to the resistance of gliomas toward lymphocyte-mediated

*Pathology and Laboratory Medicine Service, Department of Diagnostic and Molecular Medicine Health Care Group, VA Long Beach Healthcare System, Long Beach, CA 90822; †Department of Molecular Biology and Biochemistry, #Department of Biological Chemistry, **Department of Neurological Surgery, and ‡‡Department of Pathology and Laboratory Medicine, University of California, Irvine, Irvine, CA 92697; ‡Department of Cell Biology, Hoag Hospital Memorial Presbyterian Hospital Comprehensive Cancer Center, Newport Beach, CA 92658; §Chemistry and Biochemistry Department, California State University Long Beach, Long Beach, CA 90840; ¶Center for Cell and Gene Therapy, Texas Children's Cancer Center, Baylor College of Medicine, Houston, TX 77030; ‖Department of Medicine, University of Alabama at Birmingham, Birmingham, AL 35294; and ††Neuro-Oncology Program, Chao Family Comprehensive Cancer Center, University of California, Irvine, Orange, CA 92868

Received for publication May 10, 2010. Accepted for publication August 10, 2010.

This work was supported by the Veterans Affairs Medical Center (to M.R.J.), the Avon Breast Cancer Foundation via the University of California at Irvine Cancer Research Program (to M.R.J.), the Faculty-Student Collaborative Research Seed grant (to M.M.), National Institutes of Health National Institute of Neurological Disorders and Stroke Grant R21NS057341 (to L.S.L.), the American Brain Tumor Foundation Translational Research grant (to N.A.), and the University of California, Irvine, School of Medicine and Committee on Research Award (to Y.H.Z.).

Address correspondence and reprint requests to Dr. Martin R. Jadus, Box 113, Pathology and Laboratory Medicine Service, Department of Diagnostic and Molecular Medicine Health Care Group, VA Long Beach Healthcare System, 5901 East 7th Street, Long Beach, CA 90822. E-mail address: martin.jadus@va.gov

The online version of this article contains supplemental material.

Abbreviations used in this paper: AFM, atomic force microscopy; CAR-T cells, chimeric Ag-receptor–redirected T cells; DC, dendritic cell; GBM, glioblastoma multiforme; HEK, human embryonic kidney; LAK, lymphokine activated killer; LC, lymphocyte; NSLC, neural stemlike cells; rhIL-2, recombinant human IL-2.

www.jimmunol.org/cgi/doi/10.4049/jimmunol.1001526

cytotoxicity in vitro. In this study, we used atomic force microscopy (AFM) to investigate the surface topography of glioma cells. Their surfaces are revealed to be quite complex, with numerous microvilli and filopodia being present on their surfaces. These microvilli were observed on three different glioma cell lines: human U251, and rat F98 and T9 glioma cells. The F98 cells possessed short microvilli, whereas those from U251 were longer. The T9 cells displayed wavelike microridges. This cell surface complexity was not observed on mouse CT26 colon cancer cells or human embryonic kidney (HEK) cells, which had comparatively smooth surfaces. Human neurosphere cells derived from a recently isolated GBM surgical specimen also presented pleomorphic microvilli. The glioma microvilli are supported by microfilaments, because a treatment with cytochalasin B, or after cell detachment, caused these projections to recede. When the glioma cells were air-dried, the filopodia or the peripheral stretched-out microvilli revealed segmented sections with triangular, nodelike structures that allowed branching or bends in the microvilli to occur. Glioma cells were transiently depleted of their microvilli to show the immunologic significance of these microvilli. Microvilli-deficient U251 glioma cells were killed better by four different types of human cytolytic effector cells than the same U251 cells expressing the microvilli. The microvilli that penetrated through 0.4-μm pores, found within the transwell membranes, proved resistant to the actions of cytolytic lymphocytes and mechanical damage. These cell surface microstructures found on glioma cells could explain glioma invasiveness, whereas providing an unexpected resistance to lymphocyte-mediated killing.

Materials and Methods

Chemicals

Cytochalasin B was purchased from Sigma Chemical (St. Louis, MO). Wheat germ agglutinin/lectin was a gift from Dr. Brian L. Mundell, Bio-Research Products (North Liberty, IA).

Tumor cell lines and cell culture

The rat T9 and F98 cells and human U251 glioma cells have been previously described (33–35). All other tumor cells were obtained from the American Tissue Type Collection (Manassas, VA).

Human GBM samples were obtained from a patient undergoing debulking surgery at the University of California Irvine Medical Center (Orange, CA). The patient had signed an informed consent form before surgery. The tissue was kept in ice-cold saline and transported to the laboratory. The tumor was dissected and digested in 0.05% trypsin-EDTA for 30–45 min at 37˚C. This was followed by mechanical dissociation with cold dissociation buffer (DMEM/F12 containing 0.10 mg/ml DNase and 10% serum). After being filtered through a 70-μm cell strainer, the single cells were cultured in DMEM/F12 medium supplemented with 5% bovine serum on collagen-coated (2 $\mu g/cm^2$) culture plates. The primary adherent glioma culture was expanded, then subjected to nonadherent (1% agar-coated) culture conditions in serum-free DMEM/F12 medium supplemented with epidermal growth factor (20 ng/ml) and basic fibroblast growth factor (10 ng/ml), 1% B27 (Invitrogen, Carlsbad, CA) to select for expansion of neural stemlike cells (NSLCs), with changing of half the medium, twice a week. This procedure produced an NSLC population, with 100% of the cells expressing nestin. These cells will form invasive tumors when 10,000 cells are implanted into the brains of nude mice (Hu and Zhou, unpublished observations) within 6 wk. These neurosphere cells therefore resemble cancer-initiating cells/GBM stem cells.

Atomic force microscopy

Five thousand tumor cells were plated onto sterile gelatin coated coverslips within 24-well plates. The cells were allowed to adhere to the matrix for 16–18 h. Cells were fixed in 1% glutaldehyde for 30 min at 37˚C. The fixative was replaced by PBS and transported to the AFM facility at room temperature. At the AFM facility, the samples were mounted onto a J-piezo-scanner of an atomic force microscope (Nanoscope III; Digital Instruments, Santa Barbara, CA) equipped with a fluid cell. The cantilevers with oxide sharpened silicon nitride tips were 100 μm long. The images were collected in tapping height mode at frequencies of ~9.2 kHz with a scanning frequency of 1 Hz (36–38).

Electron microscopy

T9 cells were trypsinized and spun down into a pellet within a 15-ml conical centrifuge tube; this process occurred within 4 min. The supernatant was removed, and the cells were fixed at room temperature in 1 ml of a 1% glutaraldehyde-osmium phosphate fixative. The pellet was fixed for 2 d and then transferred with a spatula and embedded in Epon. The sections were cut and stained with uranyl acetate and lead citrate. The cells were visualized using a JEOL-1200EX II transmission electron microscope (Peabody, MA).

Immunofluorescence/confocal microscopy

Cells were incubated with complete tissue culture overnight (16–18 h) on sterile cover glasses within 24-well plates. The cells were fixed with 2% paraformaldehyde. Some cells were then stained to detect extracellular proteins with wheat germ agglutinin or with antibodies. Monoclonal anti-human MicA/B Ab and goat anti-perforin was obtained from Santa Cruz Biotech (Santa Cruz, CA), Mouse monoclonal anti-human her2 (c-erbB) were obtained from Lab Vision (Fremont, CA). The slides were then washed three times in PBS. After treatment with secondary fluorescein anti-rabbit Ab or Texas Red anti-goat Ab (Vector Labs, Burlingame, CA), the slides were incubated for 60 min. Finally, the cells were washed three times in PBS and mounted with ProLong Gold antifade reagent (Invitrogen). Samples were imaged using a Nikon two-laser (HeNe and Argon) PCM 2000 Confocal System on an Eclipse E800 Microscope (Melville, NY). The two different fluorescent dyes in the labeled sample were simultaneously acquired through a single illumination and detection pinhole using Compix Simple PCI software, as previously reported (33, 35). This provided exact pixel-for-pixel registration in both time and space for each dye in each channel. As a result, it can be inferred that the red-emitting and green-emitting probes are colorized when yellow areas are present in the images shown.

Immunofluorescent staining of intracranial gliomas with wheat germ agglutinin

An intracranial T9 glioma growing within an F344 rat's brain was removed from the dead animal. The tumor was located and mounted onto a cryostat. Frozen serial sections were mounted onto microscope slides. The tissue was stained with wheat germ agglutinin for 1 h at room temperature in a humidified box. The tissue was washed, and the anti-wheat germ agglutinin FITC-labeled secondary Ab was incubated for a further 1 h. The tissue was then washed and visualized on the Eclipse fluorescent microscope.

Cytolytic lymphocytes

Lymphokine activated killer cells. After informed consent forms were signed, human PBMCs were collected at Hoag Hospital, and the cells were isolated after a centrifugation using Ficoll-Hypaque. Aliquots were frozen until needed. Frozen PBMCs were thawed in a 37˚C water bath, resuspended in warm AIM-V (Life Technologies, Grand Island, NY) with antibiotics, and centrifuged at 2000 rpm for 5 min at room temperature. The cell pellet was resuspended at 3×10^6 cells/ml in AIM-V with antibiotics and supplemented in 3000 U/ml recombinant human IL-2 (rhIL-2; Chiron, Emeryville, CA). The cells were incubated in humidified air at 37˚C in 5% CO_2 for 7 d. On day 5, the cells were counted by trypan blue dye exclusion assay and resuspended in 80% fresh AIM-V at 3×10^6 cells/ml plus 3000 U/ml rhIL-2. The cell cultures exhibited typical clustering and phenotype of IL-2–activated lymphocytes, as well as cytolytic activity against NK-sensitive cell lines such as K562.

γδ T cell cultures. PBMC cultures were initiated at 1 million cells/ml and maintained in 5% CO_2 at 37˚C in RPMI-1640 with 15% autologous serum plus 1 μg zoledronic acid (Novartis Oncology, East Hanover, NJ) plus 50 U/ml rhIL-2 (Chiron) (7). Cells were initially cultured 3 ml/well in 6-well plates and transferred to T75 cm^2 flasks. Cultures are maintained for 14 d with addition of 50 U/ml rhIL-2 on postculture days 2, 6, and 10, and addition of complete media as determined by pH (phenol red) and cell density. Flow cytometry for lymphocyte subsets confirmed that the cells were consistently >80% γδ T cells.

CTLs. PBMCs were collected from an HLA-$A2^+$ donor after informed consent forms were signed at Hoag Hospital. The mononuclear cells were ficolled and then incubated in human GM-CSF (1000 U/ml) and IL-4 (1000 U/ml) in Aim-V (Life Technologies/Invitrogen, San Diego, CA) at 37˚C. The recombinant cytokines were obtained from CellGenix USA (Antioch, IL). In unpublished studies (L. Ge), by reverse transcriptase real-time PCRs, U251 cells made a very high amount of YKL-40 mRNA, and its

protein was confirmed by intracellular flow cytometry using the Quidel Corporation's antibodies (San Diego, CA). The YKL-$40_{201–210}$ peptide, SIMTYDFHGA, was synthesized by Gen Script Corporation (Piscataway, NJ). The YKL-40 peptide was incubated with the 6-d-old DCs. The immature DCs were stimulated with recombinant human TNF-α, IL-6, and IL-1β (10 ng/ml each). Mature DCs were harvested on day 8, resuspended in AIM-V medium at 10^6 cells/ml with peptide (10 μg/ml), and incubated for 2 h at 37°C. Populations of $CD8^+$ T cells, autologous to the DC donors, were enriched from PBMCs using magnetic microbeads (Miltenyi Biotech, Auburn, CA). $CD8^+$ T cells (2×10^6/well) were cocultured with peptide-pulsed DCs (2×10^5/well) in 2 ml AIM-V medium supplemented with 5% human AB serum (Invitrogen, San Diego, CA), 10 U/ml rhIL-2 (R&D Systems, Minneapolis, MN), and 10 U/ml rhIL-7 (Cell Sciences, Canton, MA) in each well of 24-well tissue culture plates. On day 15, to increase CTL frequency, we restimulated the lymphocytes with autologous DCs pulsed with peptide in AIM-V medium supplemented with 5% human AB serum (Life Technologies, San Diego, CA), rhIL-2, and rhIL-7 (10 U/ml each).

Production of HER2 CAR-T cells. Previously (34) we showed that U251 cells expressed HER2/neu by use of quantitative real-time PCR and by flow cytometry staining, so we used this receptor for a potential target of cytotoxic effector cells that had been genetically engineered to recognize this receptor (8). 293T cells were cotransfected with an FRP5.CD28.ζ retroviral vector containing plasmid, Peg-Pam-e plasmid encoding the sequence for Moloney murine leukemia virus gag-pol, and plasmid pMEVSVg containing the sequence for vesicular stomatitis virus G, using GeneJuice transfection reagent (EMD Biosciences, San Diego, CA) to produce retroviral supernatant (8). Supernatants containing the retrovirus were collected 48 and 72 h later. Vesicular stomatitis virus G pseudotyped viral particles were used to transduce the PG-13 producer cell line for the production of viral particles.

OKT3/CD28 activated T cells were transduced with retroviral vectors as described previously (8). In brief, PBMCs were isolated by Lymphoprep (Greiner Bio-One, Monroe, NC) gradient centrifugation. 5×10^5 PBMCs/well in a 24-well plate were activated with OKT3 (OrthoBiotech, Raritan, NJ) and CD28 monoclonal antibodies (BD Biosciences, Palo Alto, CA) at a final concentration of 1 μg/ml. On day 2, rhIL-2 (Chiron) was added at a final concentration of 100 U/ml, and on day 3, cells were harvested for retroviral transduction. For transduction, we precoated a nontissue culture-treated 24-well plate with a recombinant fibronectin fragment (FN CH-296; Retronectin; Takara Bio, Madison, WI). Wells were washed with PBS (Sigma, St. Louis, MO) and incubated twice for 30 min with retrovirus. Subsequently, 3×10^5 T cells/well were transduced with retrovirus in the presence of 100 U IL-2/ml. After 48–72 h, cells were removed and expanded in the presence of 50–100 U rhIL-2/ml for 10 d before use.

Cytotoxicity assay

The U251 target cells were plated (10,000 cells/well) into the wells of 96-well flat bottom plates overnight to allow them to adhere. A separate aliquot of U251 cells were detached by incubating the cells in a versene buffer for 20 min. The detached cells and the attached U251 cells were labeled with 5- (and 6-)carboxy-2′,7′-dichlorofluorescein diacetate (Molecular Probes/Invitrogen, Eugene, OR), according the manufacturer's directions. After three washes, the cells were incubated with the effector cells at either 50:1 or 12:1 effector/target cell ratios in quadruplicate cultures. Triton X-100 (1%)–treated cells served as the maximum release. U251 cells incubated without any effector cells served as the spontaneous release values. After 6 h, the supernatants were collected and analyzed on the Novostar Fluorometer/Luminometer (BMG Labtech, Offenburg, Germany) for fluorescence.

Percentage specific release was calculated as % specific release = $(\text{fluorescence}_{\text{experiment}} - \text{fluorescence}_{\text{spontaneous release}})/(\text{fluorescence}_{\text{maximum}} - \text{fluorescencespontaneous release}) \times 100$. Maximum release was determined by adding in 0.01% Triton X-100.

Data from the cytotoxicity assays were analyzed using a Student *t* test. Values were considered significantly different at $p < 0.05$ levels.

Transwell chambers

U251 glioma cells were allowed to adhere to Millipore (PICM01250) transwell chambers (Bedford, MA) for 24 h. The membrane has a pore size of 0.4 μm. The cells were then stained with wheat germ agglutinin in situ.

For cytotoxicity assays, the transwell chamber was: 1) used in standard position, so that the effector cells were in direct contact with the U251 cells; 2) inverted (with the cells attached to the chamber facing down) with the effector cells exposed to the microvilli of the U251 cells; or 3) the inverted chamber was then rubbed with a sterile cotton swab to mechanically damage the microvilli. The assay was allowed to proceed for another 6 h.

Results

Glioma cells display a complex surface topography as revealed by atomic force microscopy

U251 cells were initially examined by AFM to visualize either open or closed big potassium ion channels to continue previous studies (33). AFM utilizes a sharp imaging silicon nitride tip attached to a mechanical cantilever that physically moves over the surface of the cells. This technique allows the topology to be mapped when the cantilever/tip complex is deflected by the cell's exterior surface. One advantage of using AFM is that samples can be immediately visualized without doing any extra tissue processing.

We failed to detect any porelike BK channels on the surface of the glutaldehyde-fixed glioma cells. Instead, U251 cells showed an unexpected complex cell surface morphology that we were unaware as being present on glioma cells. Fig. 1*A* shows a representative picture of the U251 cell surface. These cells possess numerous microstructures that protrude over the cell surface that the cantilever accesses. These membrane projections were composed of either elevations or ridgelike structures with irregular twists and bends. We estimate the diameters of these raised protuberances to average at 0.4 μm. The lengths of the microridges averaged ~1.8 μm long. In our prior work using AFM (36–38), we never saw such complex cell surface microstructures on adherent cells such as NIH-3T3 fibroblasts. Human H9 $CD4^+$ lymphocytes had microvilli, but their lengths were neither as long nor as complex as those displayed by these found on the U251 cells.

We also used two additional glioma cell lines to confirm this basic observation of microvilli on U251 glioma cells. Rat glioma cells, such as F98 (Fig. 1*B*) and T9, also known as 9L (Fig. 1*C*) glioma, verified that these projections were similar to that displayed by the human U251 glioma. F98 gliomas displayed a morphology that resembled the U251 cells, except these cells had slightly shorter microvilli; the lengths averaged ~1.2 μm, with diameters of 0.3–0.4 μm. F98 cells had fewer microridges. Rat T9 glioma cells are slightly larger cells (20-μm diameters) than are U251 and F98 glioma cells (10 μm). The T9 cells instead of having individual microvilli appeared to possess microridges that randomly crisscrossed the cell surface. These structures also had irregular bends and turns. The diameters of these ridges were estimated to be between 0.4 and 0.5 μm.

The T9 glioma cells when viewed under a transmission electron microscope confirmed that these elevated structures were present. Fig. 1*D* is a cross section of T9 cells, which provides a better prospective of these microvilli. Here there are multiple microvilli extruding from T9 cells. The longest microvillus present within this micrograph was 2.8 μm long and possessed a diameter of 23 nm. We interpret the microridges seen in the AFM as long microvilli that have toppled over, either as a result of gravity or when the cantilever passed over the microvilli. Some microvilli contain branched segments.

We also imaged the cell surface of freshly isolated human GBM NSLCs to determine whether cancer-initiating cells/"stem cells" display a similar phenotype. These stemlike cells were cultured in vitro for 5 months after isolation from the patient. These cells when surgically implanted intracranially into nude mice did produce an invasive phenotype (Y. Hu and Y.H. Zhou, unpublished observations). Fig. 1*E* shows that a GBM neurosphere cell does display a complex microvilli-like structure as well. These microvilli have shorter microvilli than those displayed by the U251 cells. These microvilli and microridges appear more heterogeneous and pleomorphic. In general, these freshly isolated GBM cells have microvilli and microridges as those showed in the established glioma cell lines.

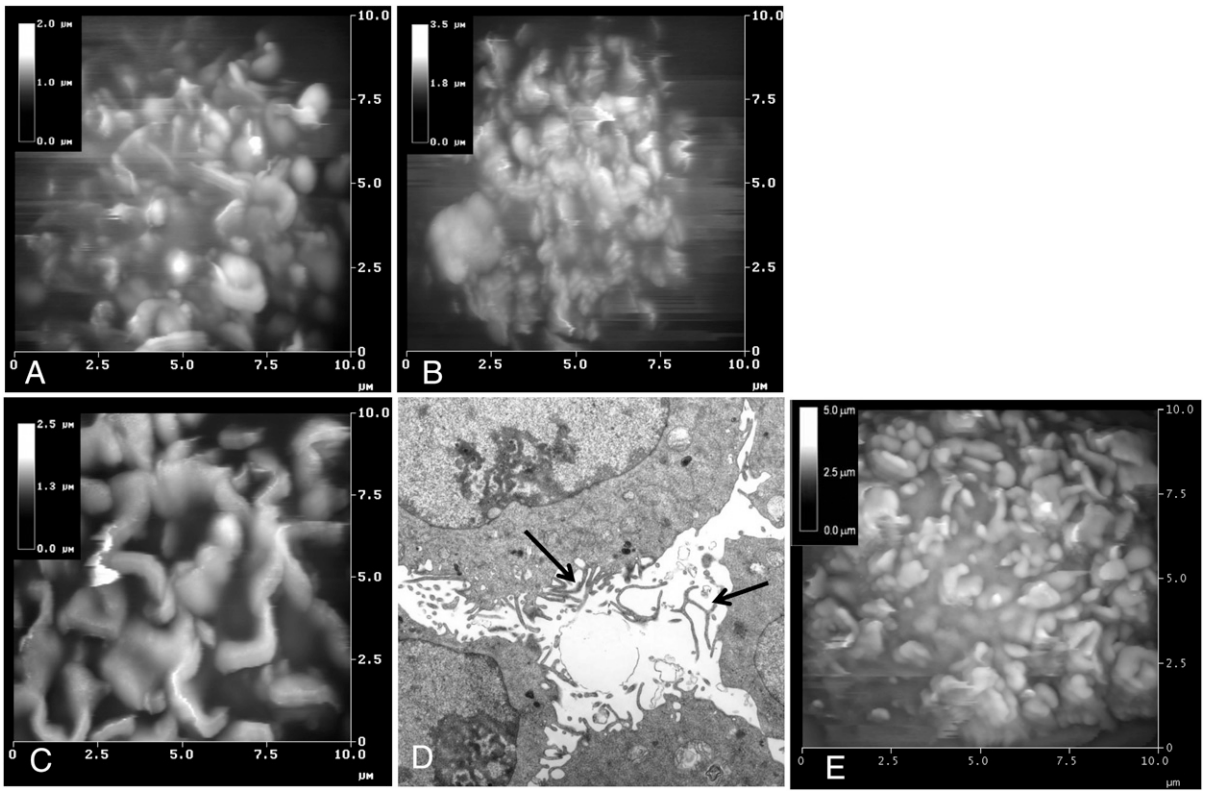

FIGURE 1. AFM of glioma cells. Glioma cells were attached to glass coverslips overnight. The next morning, the cells were fixed in 1% glutaldehyde, replaced in PBS for transport to the facility, and then imagined. *A*, Representative human U251 glioma cell. *B*, Rat F98 glioma cell. *C*, Rat T9 cell. *D*, T9 cells that were prepared for transmission electron microscopy (original magnification ×2500). Arrows show some of the longer microvilli. *E*, Freshly isolated human GBM NSLC cultured in epidermal growth factor, basic fibroblast growth factor, and B27 media, and established as neurospheres. The neurosphere cells were detached by a brief trypsinization and allowed to adhere onto a poly-D-lysine–coated coverslip for 1 h. The cells were fixed in 1% glutaldehyde and imaged.

Confocal immunofluorescence microscopy confirms that microvilli are present on glioma cells

Adherent U251 cells were stained with wheat germ agglutinin, which detects external glycoproteins (*O*-linked *N*-acetylglucosaminyl residues). Confocal microscopy was used to detect the focused fluorescence of the glycoproteins found at various heights of the cells. Fig. 2*A* shows a composite picture of different planes of the staining taken from the level of bottom of the U251 cell, where it is attached to coverslip at −4.9 μm (exposure 64, *bottom right*) to the very top of the cell at 2 μm (exposure 41, *top left*). At the top of the cell (2 μm), distinct foci of staining are seen. As the confocal focus descends downward toward the corpus of the cell, those foci (2–0.4 μm) become larger and more of them appear. We interpret the first staining to be seen are those microvilli located above the nucleus. Around the plane of the cell, another set of stains are seen above (−0.4 to −3.1 μm), then along the edge of the cells (−3.1 to −4.9 μm), where the microvilli assume a more filopodia-like morphology. These data confirm that the microvilli and filopodia are found at different three-dimensional levels of the cell.

We also made use of this wheat germ agglutinin staining to measure the height profiles of these microvilli by quantitating the fluorescence along the *z*-axis. The length (*x*-axis) and width (*y*-axis) of another U251 cell is shown in Fig. 2*B*. The height (*z*-axis) demonstrates distinct fluorescent elements are above the main body of the cell. These data confirm that the glioma possesses irregular projections above the cellular corpus. A video movie provided in Supplemental Video 1 provides a better viewing of this three-dimensional image; it shows the complex nature of these microvilli over the entire cell as the cell is rotated.

Microvilli-like structures appear within in situ intracranial T9 gliomas

T9 glioma cells were surgically implanted into an F344 rat's brain. When the tumor growth was obvious, the intracranial tumor was removed and frozen sections were cut. The sections were stained with wheat germ agglutinin. Fig. 3 shows a representative view of the glioma-normal tissue interface. The glioma cells stained heavily with the wheat germ agglutinin, whereas the normal brain tissue was only lightly stained. Within the glioma at areas that display large extracellular spaces, signs of microvilli-like structures were observed (see the circular areas on *right side*) where the gliomas reside. A similar area of extracellular space within the normal brain did not appear to possess any microvilli-like structures.

CT26 colon cancer cells and HEK cells do not possess microvilli

In contrast, mouse CT26 colon cancer cells (Fig. 4*A*) or HEK cells (Fig. 4*B*) display relatively flat surfaces devoid of any membrane elevations. The CT26 cell surface appeared to be composed of flattened plates with some elevated folds of the membrane. These plates ranged in size from 2.5 to 5 μm. In general, the majority of the membrane displayed a rather smooth surface and was free of raised microvilli that the gliomas clearly possessed. HEK cells showed a more traditional smooth area of the cell. Some elevations composed of smaller and more squarelike spikes were found at the periphery of the cell, but these spikes were distinct from those of the glioma.

Dried cells reveal a complex internal structure of the microvilli

U251 cells were allowed to air-dry and then imaged using AFM. Fig. 5*A* shows that the dried glioma possesses a rough surface. Be-

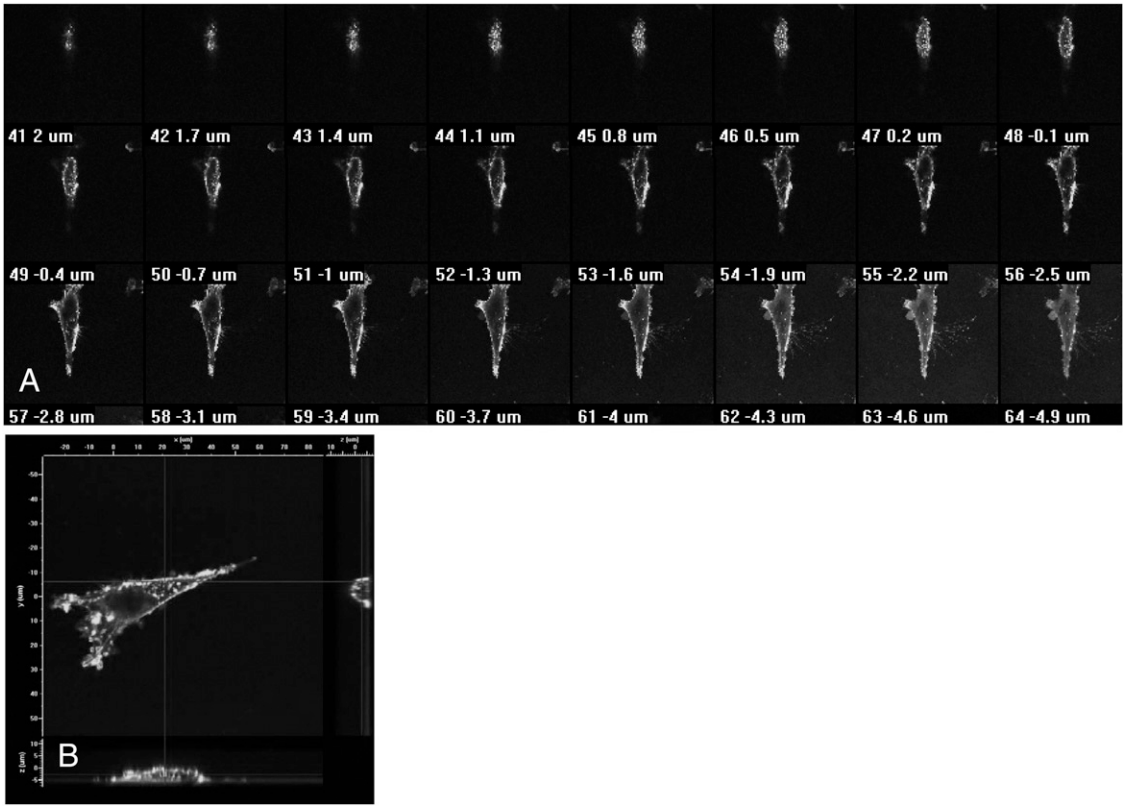

FIGURE 2. Confocal fluorescent micrograph of U251 cells showing differing microvilli. The adherent U251 cells attached overnight to coverslips, fixed, and then stained with wheat germ agglutinin, which binds extracellular proteins. The cells were washed and then visualized using a Nikon confocal microscope at various focal planes. *A*, The upper level was exposure 41 and was taken at 2 μm above the plane of the cell. Original magnification ×100. Incremental decreases in the plane of the cell were subsequently taken: exposures 41–64. *B*, Adherent U251 cells were stained with wheat germ agglutinin and then imaged under fluorescent confocal microscopy. The flat fluorescent image of the cell is shown at the *x*- and *y*-axes. The central lines provide reference points for the fluorescence shown as height of the cell on the *z*-axis for that value at both the *x*- and *y*-axes. Distinct green fluorescent microvilli can be seen on the *z*-axis.

cause most of the water is lost from air-dried cells, the entire cell is flattened and is now accessible to the AFM's cantilever along the edges of the cells. Long filopodia appear at the periphery of the cells in stringlike structures. These filopodia are presumed to be those microvilli that were located at the periphery of the cells at the time of air-drying. These projections stretch out and contain triangular nodelike structures. A higher power analysis of another cell (Fig. 5*B*) shows that these nodelike structures have an irregular repeating spacing ranging from 0.8 to 6.1 μm. These data suggest that these filopodia, and microvilli, possess some previously unknown compartmentalization within these microvillous structures.

The microvilli collapse after cytochalasin B treatment

From the electron microscopy, it appeared that the microvilli contained microfilaments. We next identified whether these glioma superstructures could collapse by depolymerization of microfilaments using cytochalasin B. T9 cells were incubated with 5 μM cytochalasin B for 30 min to disrupt the cytoskeleton. Fig. 6 shows that the microvilli and microridges previously seen to be present on T9 cells have now collapsed and the surface of these cells is now smoothed out. We conclude that these microvilli contain a cytoskeleton composed of microfilaments.

Detached U251 cells lacking the microvilli are more sensitive to cell-mediated killing than are microvilli expressing attached U251 cells

These microvilli could theoretically provide a physical barrier between the glioma's cell body and any possible effector lymphocyte. We performed experiments where Ag nonspecific effector lymphocytes, such as lymphokine activated killer (LAK) cells and γδ T cells (7), together with Ag-specific CTL and T cells engineered to possess a CAR toward the her2/neu receptor (8), could kill microvilli expressing U251 cells (Fig. 7). LAK (Fig. 7*A*) and γδ T cells (Fig. 7*B*) can bind to receptors such as ULBP1, ULBP2, ULBP3, MicA, and MicB found on gliomas (39). Because the CAR-T cells possess the ligand for the her2/neu receptor (Fig. 7*C*), allowing cell-to-cell tethering, these effector cells can specifically recognize the functional cytokine receptor and form a synapse providing the cross-linking that allows T cell–mediated killing to begin. CTLs recognize MHC class I molecules possessing the correct antigenic peptide (YKL-40 in the context of HLA-A2; Fig. 7*D*). Thus, at least three different ligand/receptor synapses were examined in these experiments. All types of effector cells were prevented from optimally killing the glioma cells when the microvilli were present in standard 6-hr cytolytic assays, although it appears that the LAK and γδ T cells are inhibited slightly better by the microvilli. At the greater E:T ratios, 50:1, killing is seen with all the target cells (nonadherent and adherent U251 cells). All cytolytic lymphocytes killed the nonadherent U251 cells significantly better ($p < 0.05$) than the microvilli-positive adherent U251 cells. Thus, these microvilli-containing cells possess a natural resistance toward various types of Ag nonspecific or Ag-specific cytolytic lymphocytes.

Receptors for the cytolytic effector cells are detected on the microvilli of the glioma

The results of the previous experiment suggested two possibilities whereby the microvilli prevent the cytolytic lymphocytes from

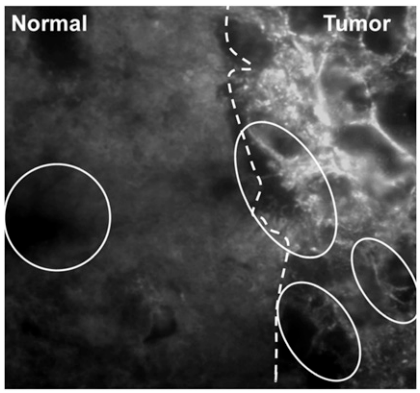

FIGURE 3. Intracranial T9 gliomas do display microvilli-like structures. T9 cells were surgically implanted into an F344 rat brain. The tumor sample was prepared as a frozen cut section. The sample was stained with wheat germ agglutinin. The glioma/normal tissue interface is shown by the well-demarcated border. The three circles on the *right* illustrate potential microvilli-like structures within the extracellular space. The *left circle* shows an extracellular space within the normal tissue that does not display any microvilli. Original magnification ×100.

killing their intended target cell. First, the microvilli are deficient in the ligands or receptors that prevent immunologic synapses from forming with the effector lymphocytes. Here these microvilli function as simple physical barriers and prevent immunologic synapses from forming. The second possibility is that the microvilli have the correct ligands that killer lymphocytes can bind, but afterward cytolysis cannot be sustained. We stained intact U251 cells for the presence of receptors that γδ T cells can recognize (MicA/B), CTLs (HLA-A2), and retargeted CAR-T cells (her2/neu) to determine whether the first possibility was valid.

Fig. 8*A* shows that the adherent U251 cells were dually stained with wheat germ agglutinin (green) to detect cell surface proteins together with the mAb directed toward her2/neu (red) and then visualized under fluorescent confocal microscopy. Cells present a yellow color where colocalization is occurring. Yellow staining was seen on the long filopodia and microvilli. There were also some areas of the glioma cell that are relatively devoid of microvilli. These microvilli-deficient regions are adjacent to the lamellipodia. At the lamellipodia there are bright areas where increased areas of her2/neu are detected.

We saw similar staining for MicA/B and HLA-A2 on the microvilli on the U251 cells (data not shown). From this evidence, the microvilli do, indeed, possess the ligands with which lymphocytic effector cells can form effective immunologic synapses.

Perforin from cytolytic effector cells incorporates into the U-251 glioma's microvilli/filopodia

We next studied whether the cytolytic lymphocytes could initiate the cytolytic process on the glioma's microvilli. All the cytolytic effector cells that we used (LAK, γδ T cells, CTLs, and CAR-T cells) use perforin and other effector molecules (i.e., granzymes, cytolysins) to kill their intended targets. We used perforin staining (red) with wheat germ agglutinin (green) to show that the microvilli were capable of accepting the pore-forming perforin molecules. CAR-T cells were incubated with the U251 cells for 60 min. Fig. 8*B* shows that perforin staining can be detected to the microvilli/filopodia where the T cell made contact with a filopodia. A three-dimensional rotational movie is provided in Supplemental Video 2, which shows the colocalization of the perforin with the microvilli, when five lymphocytes are interacting with the U251 cell. Immunofluorescent microscopy shows that perforin was incorporated into the glioma cell's filopodia/microvilli between the effector and target at the synapse.

Microvilli penetrate through transwell chamber's pores

Because the her2/neu receptor is present on the microvilli (Fig. 9), we used the CAR-T cells as the effector lymphocytes for an additional experiment. The previous experiment suggested that the microvilli might provide a natural resistance whereby the glioma is protected from the actions of cytolytic effector cells. U251 cells were allowed to adhere to the upper chamber of transwell chamber for 24 h. When the glioma cells attached themselves to the membrane of a transwell chamber, we observed that microvilli passed through the 0.4-μm pores on the basolateral side and poked through on the opposite side of the membrane (Fig. 9*A2*). Viewing the side of the transwell chamber did show that microvilli were extending into space (data not shown). Under these conditions, the corpus of the glioma cell did not transverse these pores. This observation permitted us the opportunity to prove that these exposed microvilli resist cell-mediated cytotoxicity. After glioma cell attachment to the upper membrane of the transwell chamber occurred, we flipped the chamber upside down (Fig. 9*B*). This procedure allowed only the microvilli to be exposed to the

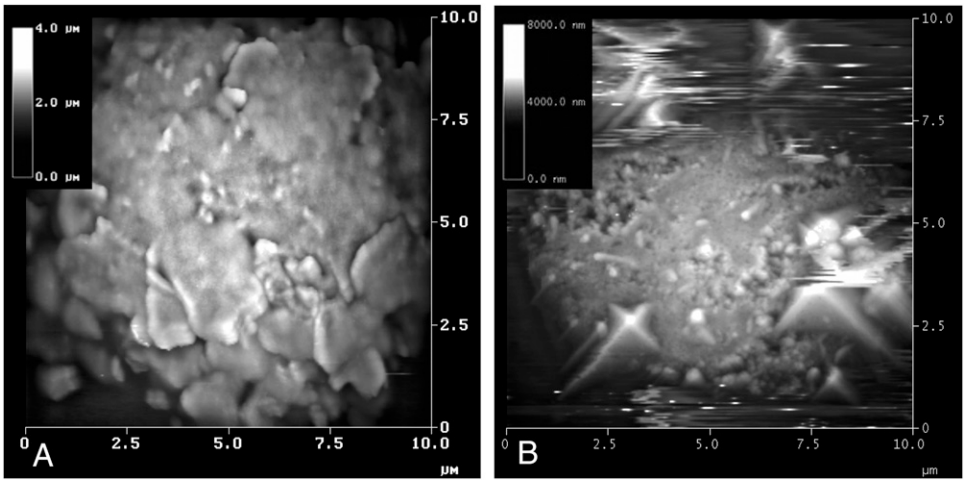

FIGURE 4. AFM of nonglioma cells show a relatively smooth cell membrane. The cells were allowed to attach themselves overnight, then fixed in 1% glutaldehyde, and then replaced with PBS. *A*, Mouse CT26 colon cancer cells. *B*, HEK cells.

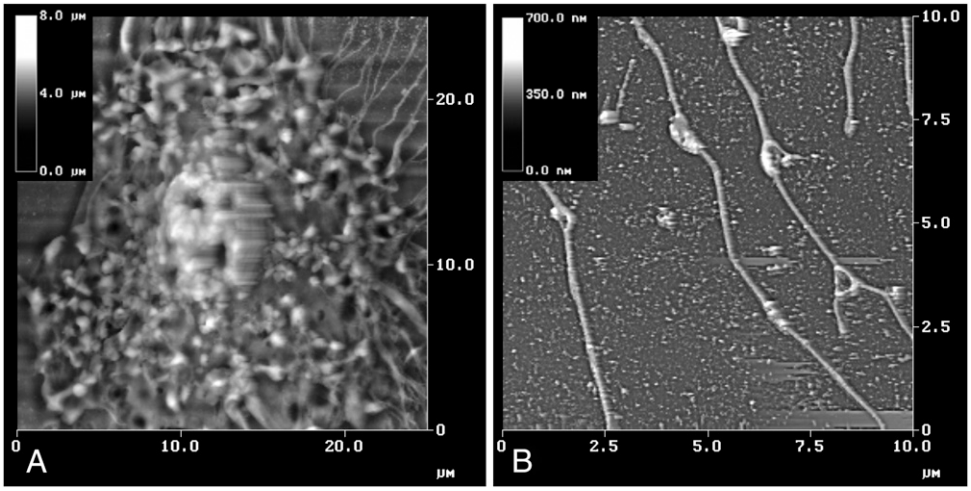

FIGURE 5. AFM of an air-dried U251 glioma cell. The glioma cells on the coverslip were allowed to air-dry overnight and then visualized under AFM. *A*, Low-power magnification of the dried U251 cell. *B*, Higher resolution image of the filopodia. These filopodia contain triangular, branching, nodelike structures.

lymphocytes. Fig. 9*C* shows that when the detached (non-attach) U251 glioma cells contacted with the CAR-T cells, excellent killing (74%) in a standard CTL assay was seen at a 50:1 E/T ratio. Simultaneously, lymphocytes that interacted with the microvilli expressing adherent U251 cells (attach) in situ on the normally positioned transwell chamber were killed to a lesser degree (37%). This confirmed our data from Fig. 7*C*. Those U251 cells that were exposed only by their microvilli (at their basolateral side) to the CAR-T cells were not significantly killed (5–8%). As a further control, we mechanically damaged the U251 microvilli (scraped) by rubbing the surface of the transwell chamber with a cotton swab to mechanically shear the microvilli. These physically damaged cells also were not killed. Thus, the glioma cells' microvilli possess a natural resistance to damage imposed by either cytolytic effector cells or mechanical damage.

Discussion

AFM allows the cell surface topography of cells to be visualized with minimal postfixative manipulation. Some artifacts are seen with this technology, because the cell surface is still flexible when the cantilever runs over the membranes. This technique can be used with living cells. When glutaldehyde-fixed glioma cells were imaged, AFM revealed a complex surface topography of glioma cells with numerous extracellular projections present on three different glioma cell lines (U251, F98, T9 in Fig. 1*A–D*) and one freshly isolated GBM NSLC (Fig. 1*E*), but not on CT26 colon cancer (Fig. 4*A*) or HEK cells (Fig. 4*B*). Transmission electron microscopy of T9 glial cells (Fig. 1*D*) confirmed that microvilli were present. Immunofluorescent confocal microscopy using wheat germ agglutinin (Figs. 2 and 8*A*), which binds to external cell surface glycoproteins, independently confirmed the presence of microvilli/filopodia. These microvilli collapsed after a brief treatment with cytochalasin B (Fig. 6), indicating that these membrane projections are microfilament based. On air-drying of the glioma cells, the peripheral filopodia contained triangular, nodelike structures (Fig. 5*B*), suggesting that there is some compartmentalization within these filopodia/microvilli. We suspect these nodal structures also produce the bends and kinks observed by AFM within the microvilli (Fig. 1).

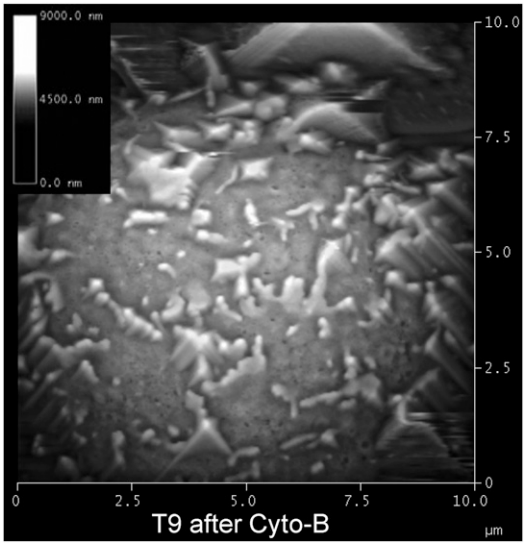

FIGURE 6. AFM of a T9 cell after cytochalasin treatment. T9 cells attached to glass coverslips overnight. The cells were treated for 30 min with cytochalasin B (cyto-B) for 30 min at 37°C. The cells were fixed in 1% glutaldehyde, replaced in PBS for transport to the facility, and then imaged.

We also saw what appeared to be microvilli within in situ intracranial gliomas (Fig. 3). When the microvilli were present, they were usually associated with cells adjacent to extracellular spaces. We did not see any microvilli within the normal brain tissue. Similar microvilli-like structures were observed within in situ human glioma using electron microscopy in Arismendi-Morillo and Castellano-Ramirez's article (Fig. 4, *top right corner*, in Ref. 40).

Microvilli/filopodia on glioma cells have been known for over 30 y, but their function or significance was never explained. Collins and colleagues (41) showed with transmission electron microscopy that at the very leading edges of membrane ruffling/lamellipodia, there were microstructures they termed either microspikes or microvilli. They also reported that the different glioma cell lines showed distinct morphologies. We examined three established glioma cell lines together with GBM NSLCs, and we saw a similar variability (long, short, and intermediate microvilli). Collins et al. also showed those triangular, nodal-like structures (Fig. 13 in Ref. 41) on the peripheral filopodia. Using scanning electron microscopy, this same group (42), together with Spence and Coates (43) and Machado et al. (44), saw similar microvilli, microridges, and filopodia on a variety of gliomas.

Hook and colleagues (32) showed by a variety of techniques (scanning electron microscopy, transmission electron microscopy,

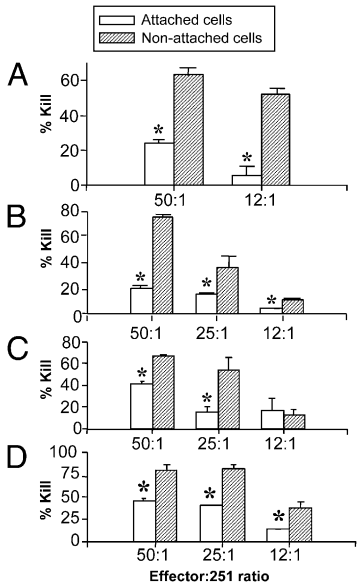

FIGURE 7. Adherent U251 cells are more resistant to the cytolytic actions of human tumoricidal effector cells. U251 cells were either labeled as attached cells (white bars) or as detached cells (hatched bars) that rounded up and lost their microvilli. The U251 cells were added to either human LAK cells (*A*), γδ T cells (*B*), CAR-T cells directed toward Her2/neu (*C*), or YKL-40–specific CTLs (*D*) at different effector/target ratios for 6 h at 37°C. Data are presented as percentage kill ± SD of quadruplicate cultures. $*p < 0.05$, statistically significantly different from its nonattached control value.

and phase-contrast microscopy), the fine details by which human LAK cells kill human SNB-92 glioma cells. This group also noted microvilli on the glioma cells. When these glioma cells were cultured within the supernatants derived from human MLRs, more microvilli on the gliomas developed. This group did not recognize that the attached cells were killed less well than the nonattached cells that were devoid of microvilli. Attached U251 cells resisted the cytolytic actions of human LAKs, conventional CTLs, CAR-T cells, or γδ T cells (Fig. 9) better than the recently detached U251 cells (which lost their microvilli). We speculate these microvilli play a role in their resistance to immune cell–mediated killing. When cancer immunologists currently do cytolytic assays with various effector cells, the adherent cancer cells including glioma cells are trypsinized or physically detached to facilitate labeling and subsequent washings of the cells with either Cr^{51} or fluorescent dyes. Once the lymphoid effectors are placed into the wells, the detached, labeled target cells, now deficit in microvilli expression, are added to the effectors. The cultures are then coincubated between 4 and 8 h. During this time, good contact is now made between the effector cells and the nonmicrovilli-positive glioma cells, allowing optimal immunologic synapses to form (Fig. 10). We postulate that normal adherent cells with intact, fully formed microvilli may interfere with this cytolytic process. Thus, this basic in vitro experimental design may be overestimating the true killing efficiency of the effector cells with the nonadherent target cells. When these ex vivo effector cells are reinfused in vivo, the glioma cells can be in their native state and are displaying microvilli, when there is available extracellular space. The tumor cells are also hiding behind various normal host stromal cells. Glioma cells are also invading the brain's parenchyma by using their microvilli to probe for openings or weak junctions between the normal cells. Once an opening is found, the glioma cell can now begin the transmigration process. Arismendi-Morillo and Castellano-Ramirez (Fig. 4, *top*, in Ref. 40) seem to show a microvilli penetrating between two adjacent cells. This is probably the spot where the killer lymphocytes will also first contact the tumor cell, because the lymphocyte is also penetrating toward the glioma. Thus, the lymphocytes may be discharging their perforin/cytotoxins into the invading microvilli of the glioma cells, which are resistant to cytolysis or mechanical damage (Fig. 9*C*), because of the compartmentalization of the microvilli (Fig. 5*B*).

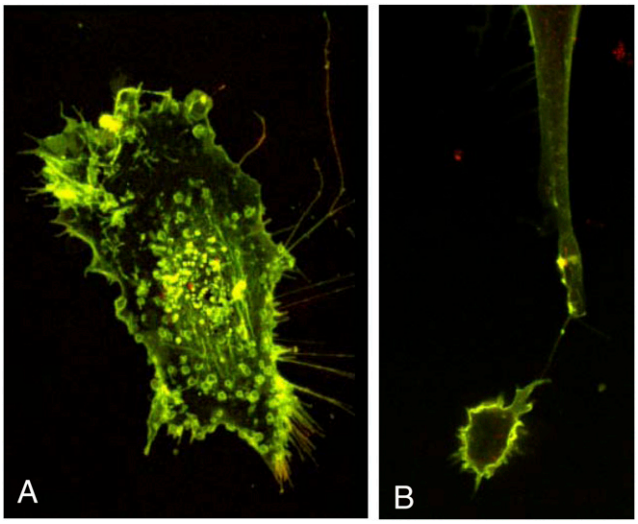

FIGURE 8. Her2 protein can be found on the microvilli and filopodia of a U251 glioma cell. *A*, Adherent U251 cells were stained with wheat germ agglutinin (green) and with the anti-Her2/neu Ab stain (red). Where yellow staining occurs, colocalization has occurred. *B*, U251 cells were allowed to incubate with CAR-T cells for 1 h at 37°C. The cells were fixed and then incubated with wheat germ lectin (green) and anti-perforin Ab (red). Original magnification ×100.

The possibility does exist that there could be other mechanisms by which adherent gliomas resist the actions of the cytolytic effector cells via the microvilli. The expression of HLA-E and HLA-G is found on human gliomas (15, 45). These molecules are capable of binding killer Ig-like receptors on T cells, NK cells, and some γδ T cells (46), and inhibit the cytolytic process. We failed to find any significant amounts of HLA-E and HLA-G expression on U251 cells (Ge, Howat, and Natividad, unpublished data). So the ability of HLA-E or HLA-G to mediate this suppression seems unlikely. Perforin is related to complement component 9 (C′9) (47). Another possibility is that gliomas possess molecules that possess membrane-bound complement regulatory proteins that could inhibit the membrane attack complex that C′9 and perforin require to form the pores that subsequently kill the target cell (48). By flow cytometry, U251 do strongly express CD46, but only minimally express CD55 and CD59 (data not shown). Work is currently in progress to determine whether CD46 can be found on the glioma microvilli.

These triangular nodes could be internal structures that allow some compartmentalization of the microvilli to occur. So if a break occurs within the invading microvilli, the cell does not die. If functional perforin pores form within the microvilli, then these nodelike structures provide a fail-safe that limits damage. We saw that when the only microvilli were exposed to cytolytic lymphocytes or physical damage, the glioma cells survived (Fig. 9*C*). Thus, cytolytic effector cells must contact regions of the cell body that are devoid of microvilli to successfully kill their target cells. When high effector/target ratios are used in vitro, some lymphocytes eventually contact those microvilli-deficient regions and kill the glioma cell. Our micrographs (Fig. 8*A*, Supplemental Video 1) do show that some small regions of the glioma cells' main body are devoid of microvilli and are still accessible to the cytolytic

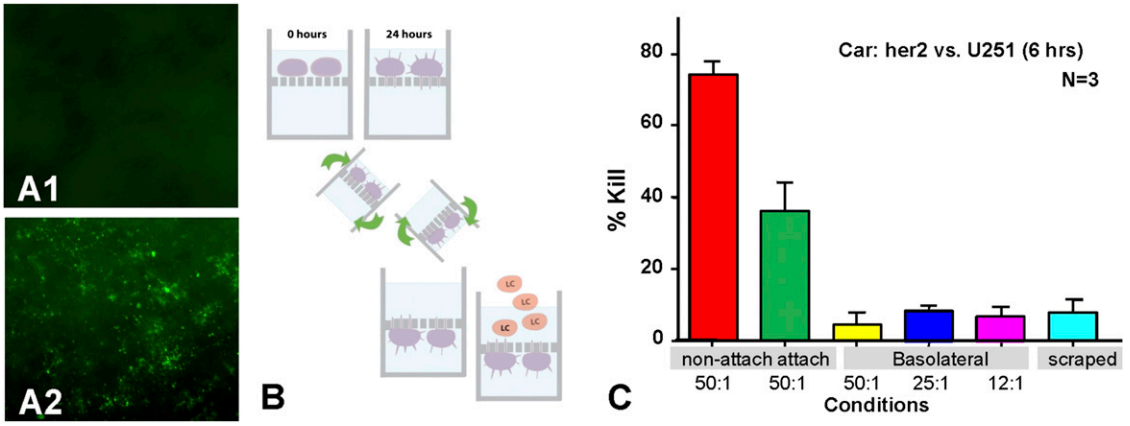

FIGURE 9. *A*, U251 cells attaching to the transwell membrane. *A1*, Negative control without any green stain; (*A2*) staining with wheat germ lectin (green) that shows discrete foci of the microvilli poking through the pores on the basolateral side of the cell. Original magnification ×40. *B*, The technique used is shown. U251 cells were allowed to adhere to the upper chamber of the transwell chamber for 24 h. Afterward, some transwell chambers were inverted so that the CAR-T lymphocytes (LC) (directed toward Her2) could interact with the microvilli that poked through the pores. *C*, Results of a cytolytic response by CAR-Her2 T cells. All samples were done in triplicate cultures. The CAR-T cells at a 50:1 ratio against nonattached U251 (red bar) are killed quite well. The CAR-T cells still can kill the attached U251 (orange bar) maintained where the lymphocytes and target cells are. Using the inverted side of the membrane (basolateral), where the lymphocytes can bind only to the U251, no killing is seen. Finally, those inverted U251 cells that were scraped by a cotton swab also failed to show any killing. The cytotoxicity assay was allowed to precede 6 h. The last four values are statistically different ($p < 0.05$) from release of the lymphocytes toward the attached U251 cells.

lymphocytes. Thus, to improve immunotherapy against GBM, we must devise strategies to defeat this natural defense provided by the gliomas' microvilli against the lymphocyte effectors. If successful therapies can be designed against these microvilli, one added benefit is that it may also target the ability of glioma cells to invade neighboring cells.

Our observation that microvilli are on attached glioma cells and are absent on nonattached glioma cells can help explain a certain empirical phenomenon seen in glioma biology. When glioma patients eventually die, sometimes their organs are donated and transplanted into recipients who need replacement organs. Occasionally, these organs possess metastatic gliomas and these secondary tumors reappear, because the organ recipients are immunosuppressed to prevent organ rejection. This is a fairly rare event, but it does occur (49, 50). The mostly likely scenario is that the glioma cells gained access to the organ via a circulating glioma cell. If this occurs, these glioma cells would be nonattached cells that we predict do not express microvilli. Therefore, these cells could be sensitive to the actions of cytolytic effector cells (CTL, NK, γδT cells, etc). Thus, these effector cells may contribute the rarity of this effect by killing the circulating glioma cells when they are most vulnerable.

Similar looking structures known as "microtentacles" have been described on breast cancer cells (51, 52). Microtentacles appear on detached breast cancer cells. It is speculated that microtentacles play a role in attaching themselves to endothelial cells as they circulate through the blood or lymph. Microtentacles are supported by an α-tubulin–based cytoskeleton; some of these microtentacles can possess τ (53). Our microvilli are shorter (1–3 μm) than the microtentacles (estimated up to 10–15 μm long). The microvilli are supported by a microfilament cytoskeleton, as opposed to the microtubules within the microtentacles. The microvilli appear when glioma cells are adherent, whereas the microtentacles form when breast cancer cells are detached. Whether these microtentacles also resist the actions of cytolytic lymphocytes remains an important, open question. This scenario could

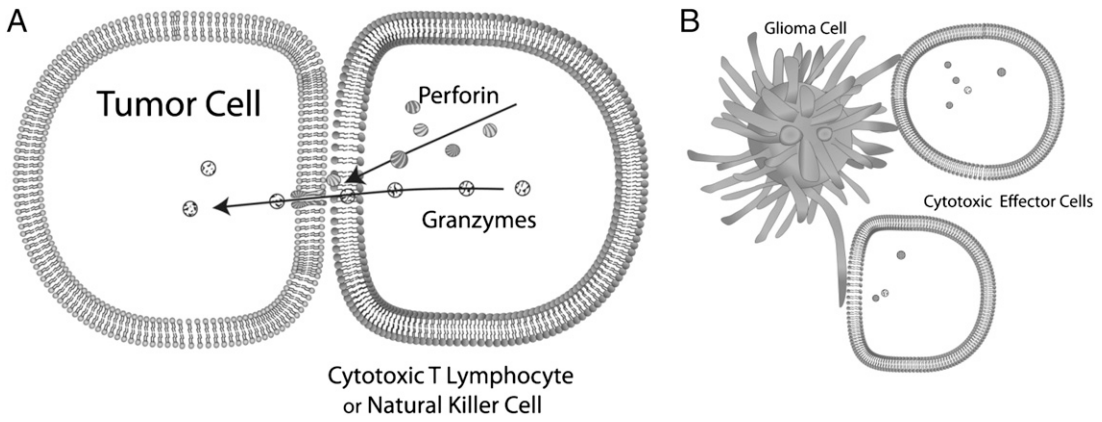

FIGURE 10. Schematic drawings that explain why the microvilli make it difficult for lymphocytes to kill adherent glioma cells. *A*, The binding of cytolytic effector cells to nonmicrovilli-expressing glioma cells after a proper immunologic synapse is formed. After a successful synapse of the glioma and the lymphocyte is made, perforin and granzymes successfully kill the glioma cells. *B*, The difficulty of the killer lymphocytes to successfully form a synapse with the corpus of the cells is shown. Either the microvilli prevent contact with the corpus of the cells or the microvilli do not allow proper perforin pore configurations to occur, because the microvilli are compartmentalized.

explain in a reverse manner why metastatic breast cancers are not readily killed by the immune system, when theoretically these individual breast cancer cells should be at their most vulnerable stage to cell-mediated lymphocytes.

The microvilli we observe on gliomas could have several roles such as increasing the cell's surface area, whereas also playing a role in invasiveness. Microvilli/microridges can increase cell surface area of the cell. Hence cell surface cytokine receptors commonly found on glioma cells (34), such as HER2/neu, EphA2, IL-13 receptor α2 (IL13Rα2), epidermal growth factor receptor and its third variant (EGFRvIII), and platelet-derived growth factor receptors could be expressed on these microvilli. We found that the HER2/neu receptors are present throughout the cell surface including on the microvilli and filopodia (Fig. 8*A*). Various growth factors do bind to extracellular matrix, so when physical wounds occur, these growth factors are released and help stimulate wound repair by fibroblasts. These growth factor receptor–enriched microvilli could help drive the glioma cell into seeking out the growth factors needed for continued stimulation. Gliomas are invasive, which undoubtedly leads to their difficulty at being treated by surgery and radiation. Hence these microvilli expressing growth factor receptors can explain this invasive nature by searching for weak spots between nontumor cells to find endogenous growth factors. Ransom and Sontheimer (54) have postulated that the leading edges of glioma cell uses the various ion channels (K^+, Na^+, and Cl^-) to penetrate and migrate through normal brain parenchymal cells by a series of swellings and contractions by these ion channels.

Finally, the presence of these microvilli and microridges helps explain why glioma cells were so difficult for us to successfully patch-clamp for the presence of functional BK ion channels in previous studies. When we patch-clamped the U251 (33) or T9 cells (35) to detect functional BK channels, we were frequently frustrated by the lack of successful membrane seals by the glass capillary. This complex topography provides a simple explanation. For a successful patch-clamp to be properly placed, the membrane must form a tight seal between the opening of the glass capillary and the membrane. These microvilli simply prevent the good seals with the membrane to occur. Previous experience in one of our laboratories (55) with HEK cells showed that these cells were extremely easy to patch-clamp. These cells possess relatively flat surfaces (Fig. 4*B*) that allowed good seals to occur with the membrane. Hence one way to improve patch-clamping of glioma cells is to first eliminate the microvilli with cytochalasin B (Fig. 6) treatment. Therefore, this observation may facilitate others who are trying to demonstrate functional ion channels on glioma cells.

In summary, we show that four different rat and human glioma cell types possess a complex surface topography with many microvilli and microridges present. When the cells were treated with cytochalasin B or became detached, these cells lost their microvilli. U251 glioma cells devoid of microvilli were more sensitive to cytolysis by four different types of human effector lymphocytes. U251 cells that were allowed to grow on transwell chambers had microvilli that penetrated the transwell pores and came out of the basolateral side. These basolateral-sided microvilli proved to be quite resistant to either cytolytic lymphocytes or mechanical damage. The significance of these structures could be quite important in explaining several aspects of glioma cell biology, and methods to disrupt these microvilli could improve immunotherapy involving cytolytic lymphocytes, as well as inhibiting glioma invasiveness.

Acknowledgments

We thank Nora Tang and Dr. Sant Sekhon for doing the transmission electron microscopy. We also thank Christiana Delgado for doing the frozen cut sectioning. We acknowledge the help of Josephine Natividad and Andrew Howat for flow cytometric analysis of U251 cells with the monoclonal anti–HLA-E and –HLA-G antibodies. We also thank the Southern California Institute for Research and Education (SCIRE) for support. We thank Dr. Linda Muul (NCI) for discussions on Glioma Topography from her previous work (32).

Disclosures

The authors have no financial conflicts of interest.

References

1. Nieder, C., A. L. Grosu, and M. Molls. 2000. A comparison of treatment results for recurrent malignant gliomas. *Cancer Treat. Rev.* 26: 397–409.
2. Hayes, R. L. 1992. The cellular immunotherapy of primary brain tumors. *Rev. Neurol. (Paris)* 148: 454–466.
3. Quattrocchi, K. B., C. H. Miller, S. Cush, S. A. Bernard, S. T. Dull, M. Smith, S. Gudeman, and M. A. Varia. 1999. Pilot study of local autologous tumor infiltrating lymphocytes for the treatment of recurrent malignant gliomas. *J. Neurooncol.* 45: 141–157.
4. Kruse, C. A., L. Cepeda, B. Owens, S. D. Johnson, J. Stears, and K. O. Lillehei. 1997. Treatment of recurrent glioma with intracavitary alloreactive cytotoxic T lymphocytes and interleukin-2. *Cancer Immunol. Immunother.* 45: 77–87.
5. Ewend, M. G., R. C. Thompson, R. Anderson, A. K. Sills, K. Staveley-O'Carroll, B. M. Tyler, J. Hanes, D. Brat, M. Thomas, E. M. Jaffee, et al. 2000. Intracranial paracrine interleukin-2 therapy stimulates prolonged antitumor immunity that extends outside the central nervous system. *J. Immunother.* 23: 438–448.
6. Plautz, G. E., D. W. Miller, G. H. Barnett, G. H. Stevens, S. Maffett, J. Kim, P. A. Cohen, and S. Shu. 2000. T cell adoptive immunotherapy of newly diagnosed gliomas. *Clin. Cancer Res.* 6: 2209–2218.
7. Bryant, N. L., C. Suarez-Cuervo, G. Y. Gillespie, J. M. Markert, L. B. Nabors, S. Meleth, R. D. Lopez, and L. S. Lamb, Jr. 2009. Characterization and immunotherapeutic potential of gammadelta T-cells in patients with glioblastoma. *Neuro-oncol.* 11: 357–367.
8. Ahmed, N., V. S. Salsman, Y. Kew, D. Shaffer, S. Powell, Y. J. Zhang, R. G. Grossman, H. E. Heslop, and S. Gottschalk. 2010. HER2-specific T cells target primary glioblastoma stem cells and induce regression of autologous experimental tumors. *Clin. Cancer Res.* 16: 474–485.
9. Doolittle, N. D., L. E. Abrey, W. A. Bleyer, S. Brem, T. P. Davis, P. Dore-Duffy, L. R. Drewes, W. A. Hall, J. M. Hoffman, A. Korfel, et al. 2005. New frontiers in translational research in neuro-oncology and the blood-brain barrier: report of the tenth annual Blood-Brain Barrier Disruption Consortium Meeting. *Clin. Cancer Res.* 11: 421–428.
10. Read, S. B., N. V. Kulprathipanja, G. G. Gomez, D. B. Paul, K. R. Winston, J. M. Robbins, and C. A. Kruse. 2003. Human alloreactive CTL interactions with gliomas and with those having upregulated HLA expression from exogenous IFN-gamma or IFN-gamma gene modification. *J. Interferon Cytokine Res.* 23: 379–393.
11. Walker, P. R., T. Calzascia, and P. Y. Dietrich. 2002. All in the head: obstacles for immune rejection of brain tumours. *Immunology* 107: 28–38.
12. Carson, M. J., J. G. Sutcliffe, and I. L. Campbell. 1999. Microglia stimulate naive T-cell differentiation without stimulating T-cell proliferation. *J. Neurosci. Res.* 55: 127–134.
13. Aloisi, F., F. Ria, G. Penna, and L. Adorini. 1998. Microglia are more efficient than astrocytes in antigen processing and in Th1 but not Th2 cell activation. *J. Immunol.* 160: 4671–4680.
14. Karman, J., C. Ling, M. Sandor, and Z. Fabry. 2004. Initiation of immune responses in brain is promoted by local dendritic cells. *J. Immunol.* 173: 2353–2361.
15. Wiendl, H., M. Mitsdoerffer, V. Hofmeister, J. Wischhusen, A. Bornemann, R. Meyermann, E. H. Weiss, A. Melms, and M. Weller. 2002. A functional role of HLA-G expression in human gliomas: an alternative strategy of immune escape. *J. Immunol.* 168: 4772–4780.
16. Smyth, M. J., S. L. Strobl, H. A. Young, J. R. Ortaldo, and A. C. Ochoa. 1991. Regulation of lymphokine-activated killer activity and pore-forming protein gene expression in human peripheral blood CD8+ T lymphocytes. Inhibition by transforming growth factor-beta. *J. Immunol.* 146: 3289–3297.
17. Inge, T. H., K. M. McCoy, B. M. Susskind, S. K. Barrett, G. Zhao, and H. D. Bear. 1992. Immunomodulatory effects of transforming growth factor-beta on T lymphocytes. Induction of CD8 expression in the CTLL-2 cell line and in normal thymocytes. *J. Immunol.* 148: 3847–3856.
18. Jachimczak, P., U. Bogdahn, J. Schneider, C. Behl, J. Meixensberger, R. Apfel, R. Dörries, K. H. Schlingensiepen, and W. Brysch. 1993. The effect of transforming growth factor-beta 2-specific phosphorothioate-anti-sense oligodeoxynucleotides in reversing cellular immunosuppression in malignant glioma. *J. Neurosurg.* 78: 944–951.
19. Wischhusen, J., M. A. Friese, M. Mittelbronn, R. Meyermann, and M. Weller. 2005. HLA-E protects glioma cells from NKG2D-mediated immune responses in vitro: implications for immune escape in vivo. *J. Neuropathol. Exp. Neurol.* 64: 523–528.
20. Hussain, S. F., D. Yang, D. Suki, K. Aldape, E. Grimm, and A. B. Heimberger. 2006. The role of human glioma-infiltrating microglia/macrophages in mediating antitumor immune responses. *Neuro-oncol.* 8: 261–279.

21. Jordan, J. T., W. Sun, S. F. Hussain, G. DeAngulo, S. S. Prabhu, and A. B. Heimberger. 2008. Preferential migration of regulatory T cells mediated by glioma-secreted chemokines can be blocked with chemotherapy. *Cancer Immunol. Immunother.* 57: 123–131.
22. Fecci, P. E., A. E. Sweeney, P. M. Grossi, S. K. Nair, C. A. Learn, D. A. Mitchell, X. Cui, T. J. Cummings, D. D. Bigner, E. Gilboa, and J. H. Sampson. 2006. Systemic anti-CD25 monoclonal antibody administration safely enhances immunity in murine glioma without eliminating regulatory T cells. *Clin. Cancer Res.* 12: 4294–4305.
23. El Andaloussi, A., and M. S. Lesniak. 2006. An increase in CD4+CD25+FOXP3 + regulatory T cells in tumor-infiltrating lymphocytes of human glioblastoma multiforme. *Neuro-oncol.* 8: 234–243.
24. Fecci, P. E., D. A. Mitchell, J. F. Whitesides, W. Xie, A. H. Friedman, G. E. Archer, J. E. Herndon, II, D. D. Bigner, G. Dranoff, and J. H. Sampson. 2006. Increased regulatory T-cell fraction amidst a diminished CD4 compartment explains cellular immune defects in patients with malignant glioma. *Cancer Res.* 66: 3294–3302.
25. Heimberger, A. B., M. Abou-Ghazal, C. Reina-Ortiz, D. S. Yang, W. Sun, W. Qiao, N. Hiraoka, and G. N. Fuller. 2008. Incidence and prognostic impact of FoxP3+ regulatory T cells in human gliomas. *Clin. Cancer Res.* 14: 5166–5172.
26. Carson, M. J., J. M. Doose, B. Melchior, C. D. Schmid, and C. C. Ploix. 2006. CNS immune privilege: hiding in plain sight. *Immunol. Rev.* 213: 48–65.
27. Constam, D. B., J. Philipp, U. V. Malipiero, P. ten Dijke, M. Schachner, and A. Fontana. 1992. Differential expression of transforming growth factor-β 1, -β 2, and -β 3 by glioblastoma cells, astrocytes, and microglia. *J. Immunol.* 148: 1404–1410.
28. Roszman, T., L. Elliott, and W. Brooks. 1991. Modulation of T-cell function by gliomas. *Immunol. Today* 12: 370–374.
29. Hishii, M., T. Nitta, H. Ishida, E. Michimasa, A. Kurosu, H. Yagita, K. Sato, and K. Okumura. 1995. Human glioma-derived interleukin-10 inhibits antitumor immune response in vitro. *Neurosurgery* 37: 1160–1167.
30. Prayson, R. A., E. A. Castilla, M. A. Vogelbaum, and G. H. Barnett. 2002. Cyclooxygenase-2 (COX-2) expression by immunohistochemistry in glioblastoma multiforme. *Ann. Diagn. Pathol.* 6: 148–153.
31. Akasaki, Y., G. Liu, N. H. C. Chung, M. Ehtesham, K. L. Black, and J. S. Yu. 2004. Induction of a $CD4^+$ T regulatory type 1 response by cyclooxygenase-2-overexpressing glioma. *J. Immunol.* 173: 4352–4359.
32. Hook, G. R., M. A. Greenwood, D. Barba, B. Ikejiri, S. N. Chen, E. H. Oldfield, R. J. Weber, and L. M. Muul. 1988. Morphology of interleukin-2-stimulated human peripheral blood mononuclear effector cells killing glioma-derived tumor cells in vitro. *J. Natl. Cancer Inst.* 80: 171–177.
33. Hoa, N., J. G. Zhang, C. Delgado, M. P. Myers, L. L. Callahan, G. Vandeusen, P. M. Schiltz, H. T. Wepsic, and M. R. Jadus. 2007. Human monocytes kill M-CSF-expressing glioma cells by BK channel activation. *Lab. Invest.* 87: 115–129.
34. Zhang, J. G., J. Eguchi, C. A. Kruse, G. G. Gomez, H. Fakhrai, S. Schroter, W. Ma, N. Hoa, B. Minev, C. Delgado, et al. 2007. Antigenic profiling of glioma cells to generate allogeneic vaccines or dendritic cell-based therapeutics. *Clin. Cancer Res.* 13: 566–575.
35. Hoa, N., M. P. Myers, T. G. Douglass, J. G. Zhang, C. Delgado, L. Driggers, L. L. Callahan, G. VanDeusen, J. T. Pham, N. Bhakta, et al. 2009. Molecular mechanisms of paraptosis induction: implications for a non-genetically modified tumor vaccine. *PLoS ONE* 4: e4631.
36. Kuznetsov, Y. G., S. Datta, N. H. Kothari, A. Greenwood, H. Fan, and A. McPherson. 2002. Atomic force microscopy investigation of fibroblasts infected with wild-type and mutant murine leukemia virus (MuLV). *Biophys. J.* 83: 3665–3674.
37. Kuznetsov, Y. G., J. G. Victoria, A. Low, W. E. Robinson, Jr., H. Fan, and A. McPherson. 2004. Atomic force microscopy imaging of retroviruses: human immunodeficiency virus and murine leukemia virus. *Scanning* 26: 209–216.
38. Kuznetsov, Y. G., J. G. Victoria, W. E. Robinson, Jr., and A. McPherson. 2003. Atomic force microscopy investigation of human immunodeficiency virus (HIV) and HIV-infected lymphocytes. *J. Virol.* 77: 11896–11909.
39. Friese, M. A., M. Platten, S. Z. Lutz, U. Naumann, S. Aulwurm, F. Bischof, H. J. Bühring, J. Dichgans, H. G. Rammensee, A. Steinle, and M. Weller. 2003. MICA/NKG2D-mediated immunogene therapy of experimental gliomas. *Cancer Res.* 63: 8996–9006.
40. Arismendi-Morillo, G. J., and A. V. Castellano-Ramirez. 2008. Ultrastructural mitochondrial pathology in human astrocytic tumors: potentials implications pro-therapeutics strategies. *J. Electron Microsc. (Tokyo)* 57: 33–39.
41. Collins, V. P., U. T. Brunk, B. A. Fredriksson, and B. Westermark. 1979. The fine structure of growing human glia and glioma cells. *Acta Pathol. Microbiol. Scand A* 87: 29–36.
42. Collins, V. P., N. Forsby, U. T. Brunk, and B. Westermark. 1977. The surface morphology of cultured human glia and glioma cells. A SEM and time-lapse study at different cell densities. *Cytobiologie* 16: 52–62.
43. Spence, A. M., and P. W. Coates. 1978. Scanning electron microscopy of cloned astrocytic lines derived from ethylnitrosourea-induced rat gliomas. *Virchows Arch. B Cell. Pathol.* 28: 27–35.
44. Machado, C. M. L., A. Schenka, J. Vassallo, W. Tamashiro, E. M. Gonçalves, S. C. Genari, and L. Verinaud. 2005. Morphological characterization of a human glioma cell line. *Cancer Cell Int.* 5: 13–22.
45. Mittelbronn, M., P. Simon, C. Löffler, D. Capper, B. Bunz, P. Harter, H. Schlaszus, A. Schleich, G. Tabatabai, B. Goeppert, et al. 2007. Elevated HLA-E levels in human glioblastomas but not in grade I to III astrocytomas correlate with infiltrating CD8+ cells. *J. Neuroimmunol.* 189: 50–58.
46. Barakonyi, A., K. T. Kovacs, E. Miko, L. Szereday, P. Varga, and J. Szekeres-Bartho. 2002. Recognition of nonclassical HLA class I antigens by gamma delta T cells during pregnancy. *J. Immunol.* 168: 2683–2688.
47. Tschopp, J., D. Masson, and K. K. Stanley. 1986. Structural/functional similarity between proteins involved in complement- and cytotoxic T-lymphocyte-mediated cytolysis. *Nature* 322: 831–834.
48. Mäenpää, A., S. Junnikkala, J. Hakulinen, T. Timonen, and S. Meri. 1996. Expression of complement membrane regulators membrane cofactor protein (CD46), decay accelerating factor (CD55), and protectin (CD59) in human malignant gliomas. *Am. J. Pathol.* 148: 1139–1152.
49. Collignon, F. P., E. C. Holland, and S. Feng. 2004. Organ donors with malignant gliomas: an update. *Am. J. Transplant.* 4: 15–21.
50. Armanios, M. Y., S. A. Grossman, S. C. Yang, B. White, A. Perry, P. C. Burger, and J. B. Orens. 2004. Transmission of glioblastoma multiforme following bilateral lung transplantation from an affected donor: case study and review of the literature. *Neuro-oncol.* 6: 259–263.
51. Whipple, R. A., A. M. Cheung, and S. S. Martin. 2007. Detyrosinated microtubule protrusions in suspended mammary epithelial cells promote reattachment. *Exp. Cell Res.* 313: 1326–1336.
52. Whipple, R. A., E. M. Balzer, E. H. Cho, M. A. Matrone, J. R. Yoon, and S. S. Martin. 2008. Vimentin filaments support extension of tubulin-based microtentacles in detached breast tumor cells. *Cancer Res.* 68: 5678–5688.
53. Matrone, M. A., R. A. Whipple, K. Thompson, E. H. Cho, M. I. Vitolo, E. M. Balzer, J. R. Yoon, O. B. Ioffe, K. C. Tuttle, M. Tan, and S. S. Martin. 2010. Metastatic breast tumors express increased tau, which promotes microtentacle formation and the reattachment of detached breast tumor cells. *Oncogene* 29: 3217–3227.
54. Ransom, C. B., and H. Sontheimer. 2001. BK channels in human glioma cells. *J. Neurophysiol.* 85: 790–803.
55. Myers, M. P., J. Yang, and P. Stampe. 1999. Visualization and functional analysis of a BK channel (*mSlo*) fused to green fluorescent protein (GFP). *Electron. J. Biotechnol.* 2: 3.